



OXFORD CENTRE FOR COLLABORATIVE APPLIED MATHEMATICS

Report Number 10/26

On an evolution equation for sand dunes

by

A. S. Ellis and A. C. Fowler



Oxford Centre for Collaborative Applied Mathematics
Mathematical Institute
24 - 29 St Giles'
Oxford
OX1 3LB
England

On an evolution equation for sand dunes

A. S. Ellis

Mathematical Institute, 24–29 St. Giles',
Oxford, U. K.

A. C. Fowler

MACSI, Dept. of Mathematics and Statistics,
University of Limerick,
Limerick, Ireland.

June 15, 2010

Abstract

We propose a model for aeolian or fluvial dune formation in which the turbulent flow of air or water is described by a constant eddy viscosity model. Asymptotic methods are used to derive an expression for the basal shear stress and this is used in the Exner equation to describe a nonlinear model for the evolution of dunes. The model is then extended to allow for the existence of separation bubbles in a self-consistent way, and computational results of the consequent model are presented.

1 Introduction

There is a very large literature on the mathematical modelling of sand dune formation. The subject started in earnest with the work of Bagnold [2] in the 1940s, who studied in detail the mechanisms by which sand is transported in deserts. The first theoretical model for dune formation is that due to Kennedy [14], who showed that an upstream shift of the maximum shear stress in flow over a wavy boundary, which had earlier been demonstrated by Benjamin [3], caused an instability to occur in a potential flow model. Engelund [8] and Smith [31] took an alternative approach, both assuming a turbulent fluid flow described by a constant eddy viscosity. Engelund found conditions for the formation of both dunes and anti-dunes (at high Froude number), in the latter case when suspended sediment was included in the model. Smith limited himself to the consideration of bedload transport. Thus they both focussed primarily on fluvial dunes, and their stability results were numerical, precluding a simple progress to finite amplitude calculations. Subsequent developments of the instability theory were made by Fredsøe [11], Richards [27] (who extended the theory to the formation of ripples), Sumer and Bakioglu [32], Colombini [5] and Charru and Hinch [4].

Although the linear instability theory of dune (and ripple) formation is thus well developed, the nonlinear theory is less so. In order to develop an efficient nonlinear theory, one needs to be able to parameterise the shear stress (and thus the sand transport) due to air flow over a bumpy topography. Ideally this should be done analytically, so that one can provide a closed model based on the Exner equation of sand transport. In the case of laminar flow at high Reynolds number, one can develop the boundary layer theory for the solution of the Orr-Sommerfeld equation [3], [30] to provide such descriptions, and one can also use this solution if the flow is turbulent, with an assumed constant eddy viscosity [10]. In the more realistic situation where the flow is turbulent but the eddy viscosity is described using a mixing length theory, approximate descriptions of the flow have been developed by Jackson and Hunt [13] and Hunt *et al.* [12], and these have been successfully used by Hermann and co-workers to simulate various kinds of dune [16], [26]. One can also solve the air (or water) flow problem directly by numerical means, and this has been done by Parsons *et al.* [24], [23], who also compare their results to experiment. Such computational results do not lend themselves easily to effective models of dune evolution, however.

The principal difficulty that finite amplitude dune theories face is that dunes almost invariably develop a slip face at their rear, where the fluid flow separates, forming a separation bubble. The description of this bubble is thus of some interest. To date, the only way in which the separation bubble has been included in models is by an *ad hoc* assumption of its shape [16]. One of the goals of dune modelling is therefore to eradicate this deficiency, and this forms a primary aspiration of the present study. Apart from the *ad hoc* nature of the treatment of the separation bubble by Kroy *et al.* [16], there is another difficulty which has not yet been pointed out. The approximate formula for the basal shear stress, based on the Jackson-Hunt formula, assumes an attached flow everywhere. When separation occurs, this formula can no longer be used. This does not appear to have been commented on previously. The issue of the description of the separation bubble thus involves two adjustments: how to deal with the separated free boundary, and how to recompute the basal shear stress formula for separated flow. In the present paper, we will attempt to address the first of these problems. Solution of the second is reserved for future work.

There has been a proliferation of interest in this subject in recent years. The stress due to varying topography is either calculated using the Jackson-Hunt [12] mixing length theory, as for example by [16] and [28], or the Benjamin [3] constant viscosity theory, as for example by [10], [9] and [15]. Langlois and Valance [17], [18] and Valance and Langlois [33] also use the constant viscosity model in a stability analysis, although supposing that the flow is laminar. These authors [19] also study the formation of ripples under (turbulent) water flow experimentally, and note the fact that the developing ripples coarsen as they evolve, a fact also noted by Ouriemi *et al.* [22] in their experiments on dune formation in a pipe flow.

The instability in the Hunt model arises through the fact that the perturbed stress has a component proportional to the surface slope, and this provides a negative diffusion term in the Exner equation which describes sand transport. In the Benjamin theory, the stress is a convolution of a kernel function with the upstream slope, as we show below, and this also leads to instability. In both cases, the resulting unbounded growth rate at infinite wave numbers is limited either by the finite saturation length of sand transport [28], as discussed by Andreotti *et al.* [1], or by the effect of gravity on sand transport [11], and there is a consequent preferred, fastest growing wavelength. While the importance of the saturation length for aeolian saltation is clear from Bagnold's [2] work, it is less relevant to

fluvial dunes, where bedload transport dominates at low Froude number, and the relaxation length may be only a few grain diameters [1], but the finite thickness of the bedload layer itself may be important [4].

Some of the models have been applied to specific types of dunes. Schwämmle and Herrmann [29] applied the Jackson–Hunt model to transverse dunes in three dimensions and Parteli *et al.* [25] have applied it to barchan dunes. More recently, Parteli *et al.* [26] have studied seif dunes formed under the action of bimodal winds. As noted above, these papers describe separation in a reasonable but *ad hoc* way.

Our aim in this paper is to develop the constant viscosity theory of dunes. In particular, we will develop, within this theoretical framework, a computational procedure which for the first time allows us to compute the flow in the presence of a separation bubble. Some parts of this analysis have been stated before, but without derivation [10], [9]. We consider a two-dimensional turbulent flow of fluid of a finite depth over an erodible bed. The model is most pertinent to transverse dunes, these having a cross-section which is essentially laterally invariant. The bed evolution is governed by the Exner equation and throughout the bedload is assumed to be saturated. Perturbations to the flow due to basal undulations are described by the Orr-Sommerfeld equation, from which it is possible to determine a formula for the basal shear stress. We see that this formula provides an instability which can describe dune formation. The instability is stabilised at high wave numbers by the downslope component of the driving shear stress. The nonlinear evolution of the resulting dune is studied computationally, with a particular view to evaluating the effect of lee side separation on the dune evolution, thus avoiding the *ad hoc* approach adopted by [1] and [16], for example.

The structure of the paper is as follows. Section 2 deals with the governing equations and the basic modelling. The derivation of the shear stress is derived in section 3. The linear stability analysis is presented in section 4. We show that disturbances can grow and propagate, and that large wavenumber disturbances can be stabilised. An evolution equation is derived in section 5, which allows for the extension of the model to include the effects of separation, and computational results are presented. Concluding remarks follow in section 6. An appendix is included where the asymptotics of the Orr-Sommerfeld equation are presented for reference.

2 The governing equations

We consider a two-dimensional fluid flow over an erodible bed as in figure 1. In a fluvial setting the upper surface is the free surface of the river; in an aeolian setting the upper surface is taken to be the top of the planetary boundary layer. The upper surface of the fluid has a height of $z^* = \eta^*(x^*, t^*)$, relative to a reference level which is the undisturbed sand surface, where z^* is the vertical spatial coordinate, x^* is the horizontal spatial coordinate and t^* is time. (Here and throughout an asterisk denotes a dimensional quantity, absence of an asterisk denotes a nondimensional quantity.) The surface of the bed is located at $z^* = s^*(x^*, t^*)$ and therefore the depth of the fluid layer is given by

$$h^* = \eta^* - s^*. \quad (1)$$

Mass conservation of the erodible substrate in the bed is described by the Exner equation,

$$(1 - n) \frac{\partial s^*}{\partial t^*} + \frac{\partial q^*}{\partial x^*} = 0 \quad (2)$$

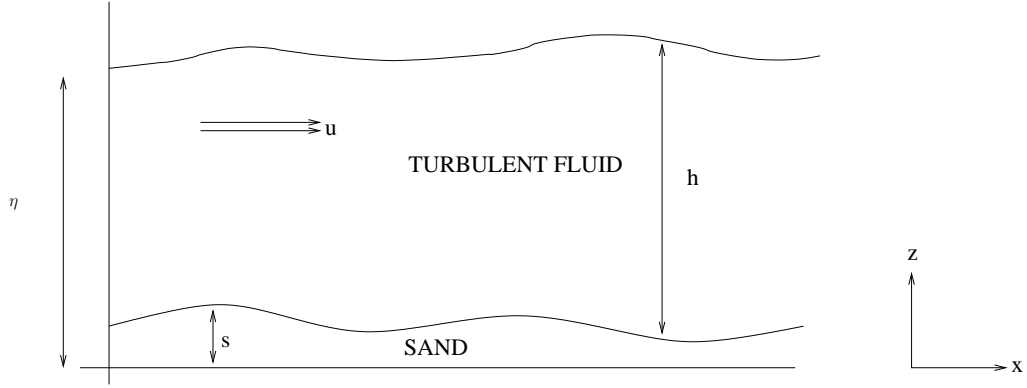


Figure 1: Sketch of the flow geometry. Vertical distances are measured from an arbitrary reference level.

where n is the porosity of the substrate and q^* is the bedload transport rate. The bedload transport q^* is related to the basal shear stress τ^* by the Meyer-Peter and Müller law [21],

$$q^* = C_{MPM} (\tau^* - \tau_c^*)_+^{3/2} \quad (3)$$

where τ_c^* is a critical basal shear stress for transport to occur, $x_+ = \max(x, 0)$ and C_{MPM} is a constant. The bedload transport, which determines the mass of sand that is transported along the bed, is considered to be saturated. The basal shear stress for a uniform flow is assumed to satisfy the empirical friction law

$$\tau^* = f \rho_f^* \bar{u}^{*2} \quad (4)$$

where ρ_f^* is the density of water, f is the Prandtl friction factor, and \bar{u}^* is the depth-averaged horizontal velocity in a uniform flow. This relation will be modified for a non-uniform flow, as described in section 3, and is dependent upon a suitable definition of the eddy viscosity

The momentum equations of the fluid flow are the turbulent Navier-Stokes equations

$$u_{t^*}^* + u^* u_{x^*}^* + w^* u_{z^*}^* = -\frac{1}{\rho_f^*} p_{x^*}^* + \nu_T^* \nabla^2 u^* + g^* S, \quad (5)$$

$$u_{t^*}^* + u^* w_{x^*}^* + w^* w_{z^*}^* = -\frac{1}{\rho_f^*} p_{z^*}^* + \nu_T^* \nabla^2 w^* - g^*, \quad (6)$$

where we suppose that the Reynolds stresses are related to the mean strain rate tensor through a constant eddy viscosity ν_T^* , determined below. Also, p^* is the pressure, g^* is the acceleration due to gravity, and $S = \sin \theta$ where θ is the inclination of the bed to the horizontal. The gravity term in (6) is strictly $g^*(1 - S^2)^{1/2}$, but the difference is small for small slopes and is in any case easily altered to the form in (5) and (6) by mild redefinition of S and g^* .

Mass conservation of the fluid is expressed by the incompressibility condition,

$$u_{x^*}^* + w_{z^*}^* = 0. \quad (7)$$

Integration of this over the depth yields

$$h_{t^*}^* + (h^* \bar{u}^*)_{x^*} = 0. \quad (8)$$

The prescription in (5) and (6) is appropriate for a sloping bed, as for example in a river. In the case of aeolian dunes, there is no slope, but the flow is driven, if we suppose the eddy-viscous fluid occupies the planetary boundary layer, by a superimposed atmospheric velocity, much as in a Blasius boundary layer. Ultimately, this tropospheric flow is driven by the slope of the tropopause, which has the effect of producing a pressure gradient on the boundary layer flow, and in effect the form of the equations is the same, the downslope gravity term being replaced by a constant pressure gradient.

The equations are nondimensionalised as follows. We suppose that h_0^* is the depth of the fluid (in the undisturbed state), u_0^* is the mean velocity of the fluid in the undisturbed uniform state, $\tau_0^* = f^* \rho_f^* u_0^{*2}$ is the consequent stress given by (4), and q_0^* is a characteristic value of the bedload flux. Then we put $h^* = h_0^* h$, $\eta^* = h_0^* \eta$ and $s^* = h_0^* s$; also $x^* = h_0^* x$, $q^* = q_0^* q$, $\tau^* = \tau_0^* \tau$, $p^* = \rho_f^* u_0^{*2} p$, $u^* = u_0^* u$ and $w^* = u_0^* w$, so that the convective timescale for the flow is $t_0^* = (1 - n) h_0^{*2} / q_0^*$. Thus

$$h = \eta - s, \quad (9)$$

determines the nondimensional depth of the fluid. The nondimensional Exner equation is

$$s_t + q_x = 0. \quad (10)$$

Assuming that $\tau^* \gg \tau_c^*$, the Meyer-Peter Müller law becomes

$$q = \tau^{3/2}, \quad (11)$$

provided that $q_0^* = C_{MPM} \tau_0^{*3/2}$. The turbulent Navier-Stokes equations nondimensionalise in the usual manner to the form

$$\varepsilon u_t + uu_x + wu_z = -p_x + \frac{1}{\text{Re}_T} \nabla^2 u + \frac{S}{\text{Fr}^2}, \quad (12)$$

$$\varepsilon w_t + uw_x + ww_z = -p_z + \frac{1}{\text{Re}_T} \nabla^2 w - \frac{1}{\text{Fr}^2}, \quad (13)$$

$$u_x + w_z = 0, \quad (14)$$

where $\text{Re}_T = u_0^* h_0^* / \nu_T^*$ is the turbulent Reynolds number, $\text{Fr} = u_0^* / \sqrt{g^* h_0^*}$ is the Froude number and where $\varepsilon = q_0^* / (1 - n) h_0^* u_0^*$ represents the ratio of the bedload flux to the fluid flux. Finally, the integrated conservation of mass equation becomes

$$\varepsilon h_t + (h\bar{u})_x = 0. \quad (15)$$

From Dong *et al.* [6] we find that a typical value for aeolian sand transport is $q_0^* = 4 \times 10^{-5} \text{ m}^2 \text{ s}^{-1}$. Taking typical atmospheric values $u_0^* = 10 \text{ m s}^{-1}$, $h_0^* = 600 \text{ m}$ and $n = 0.4$, we find that $\varepsilon \sim 10^{-8} \ll 1$. Therefore the fluid flow is quasi-stationary; the same is true in the fluvial case.

2.1 Basic velocity profile

Having derived the governing equations, we now describe the basic Poiseuille profile of the flow, independent of x . The boundary conditions are those of no stress and constant (zero)

pressure at the top surface $z = \eta$, and no slip at the base $z = s$, and we take both s and η to be constant, with $\eta = 1$, $s = 0$. The pressure is hydrostatic, so

$$p = \frac{1 - z}{\text{Fr}^2}, \quad (16)$$

while the velocity profile is

$$u = \frac{S\text{Re}_T}{\text{Fr}^2} \left[z - \frac{1}{2}z^2 \right], \quad (17)$$

and consequently the depth-averaged velocity is

$$\bar{u} = \frac{S\text{Re}_T}{3\text{Fr}^2} = 1, \quad (18)$$

by choice of the velocity scale. Hence u_0^* satisfies

$$gSh_0^{*2} = 3\nu_T^*u_0^*. \quad (19)$$

The velocity profile in the basic state can thus be written in the form

$$u = 3 \left[z - \frac{1}{2}z^2 \right]. \quad (20)$$

Now we must reconcile the assumption that the basal stress is given by the empirical equation (4) with its direct computation from the velocity profile (20). For these to be equivalent, we require

$$\rho_f^* f \bar{u}^{*2} = \rho_f^* \nu_T^* \left. \frac{\partial u^*}{\partial z^*} \right|_{z^*=s^*}, \quad (21)$$

and after some algebra, we find that this is the case if the eddy viscosity is of the form

$$\nu_T^* = \frac{1}{3} f u_0^* h_0^*, \quad (22)$$

and this is consistent with common prescriptions for ν_T .

3 The perturbed basal shear stress

We now wish to study a perturbed flow about a uniform state. We take the uniform state to be as described above, with depth $h = 1$, base at $s = 0$, and a top surface at $\eta = 1$. We denote the velocity profile in the basic state (20) as $U(z)$,

$$U(z) = 3 \left(z - \frac{1}{2}z^2 \right). \quad (23)$$

We can suppose that the bed is immobile, and we will suppose that s is small, so that the perturbations are small. Eliminating the pressure terms from (12) and (13), and defining a perturbation stream function ψ by

$$u = U(z) + \psi_z, \quad w = -\psi_x, \quad (24)$$

we derive the linearised Orr-Sommerfeld equation for ψ ,

$$U \nabla^2 \psi_x - U'' \psi_x = \frac{1}{\text{Re}_T} \nabla^4 \psi. \quad (25)$$

It is important to note that in doing this, we assume that ν_T^* is constant. In view of (22), this implies that the volume flux in the perturbed state is the same as that in the basic state. This has an implication for the boundary conditions for (25).

The linearised boundary conditions are as follows. Zero pressure at the surface $z = \eta$ provides

$$p|_{z=1} \approx (1 - \eta) p_z|_{z=1}, \quad (26)$$

i. e.,

$$\eta \approx 1 + \text{Fr}^2 p|_{z=1}. \quad (27)$$

We choose now to consider only placid flow at small Froude numbers $\text{Fr} \ll 1$, so

$$\eta \approx 1. \quad (28)$$

The no-slip condition $u|_{z=s} = 0$ on $z = s$ yields

$$\psi_z|_{z=0} = -sU'(0). \quad (29)$$

The condition of no stress on the upper surface $u_z|_{z=\eta} = 0$ gives

$$\psi_{zz}|_{z=1} = 0. \quad (30)$$

As mentioned above, the volume flux of the flow is the same as that over the unperturbed bed. Hence, we can take

$$\psi|_{z=0} = \psi|_{z=1} = 0. \quad (31)$$

In summary we must solve the Orr-Sommerfeld equation (25) subject to the boundary conditions

$$\psi = 0 \quad \text{on} \quad z = 0, \quad (32a)$$

$$\psi_z = -sU'(0) \quad \text{on} \quad z = 0, \quad (32b)$$

$$\psi = 0 \quad \text{on} \quad z = 1, \quad (32c)$$

and

$$\psi_{zz} = 0 \quad \text{on} \quad z = 1. \quad (32d)$$

The dimensionless basal shear stress for the perturbed flow is given approximately by

$$\tau = \frac{\rho_f^* \nu_T \frac{\partial u^*}{\partial z^*} \Big|_{z^*=s^*}}{\tau_0^*} = \frac{1}{3} \frac{\partial u}{\partial z} \Big|_{z=s}, \quad (33)$$

using $\tau_0^* = \rho_f^* f u_0^{*2}$, together with the definition of ν_T in (22). In terms of ψ , this can be written in the approximate form, correct to terms of $O(s)$,

$$\tau = \frac{1}{3} (U'(0) + sU''(0) + \psi_{zz}|_{z=0}). \quad (34)$$

In order to fully specify the basal shear stress we are required to determine $\psi_{zz}|_{z=0}$. Thus, seeking solutions for ψ we first take the Fourier transform of the Orr-Sommerfeld equation (25) and of the boundary conditions (32), defining the Fourier transform as

$$\mathcal{F}(u(x)) = \hat{u}(k) = \int_{-\infty}^{\infty} u(x) e^{-ikx} dx. \quad (35)$$

In addition we define Ψ by

$$\hat{\psi} = -\hat{s}U'(0)\Psi. \quad (36)$$

Thus we have to solve

$$ik [U (-k^2\Psi + \Psi'') - U''\Psi] = \frac{1}{\text{Re}_T} \left(k^4\Psi - 2k^2\Psi'' + \Psi^{(iv)} \right), \quad (37)$$

subject to

$$\Psi''(1, k) = 0, \quad (38a)$$

$$\Psi(1, k) = 0, \quad (38b)$$

$$\Psi(0, k) = 0, \quad (38c)$$

and

$$\Psi'(0, k) = 1. \quad (38d)$$

Then $\psi_{zz}|_{z=0}$ is given by the inverse Fourier transform of $-\hat{s}U'(0)\Psi''|_{z=0}$, i. e.,

$$\psi_{zz}|_{z=0} = -\frac{U'(0)}{2\pi} \int_{-\infty}^{\infty} \hat{s}' \frac{\Psi''(0, k)}{ik} e^{ikx} dk, \quad (39)$$

where we have also used the fact that $\hat{s}' = ik\hat{s}$. Using the convolution theorem, it is straightforward to obtain

$$\psi_{zz}|_{z=0} = U'(0) \int_{-\infty}^{\infty} s'(\xi) K(x - \xi) d\xi \quad (40)$$

where the convolution kernel $K(x)$ has the Fourier transform

$$\hat{K}(k) = -\frac{\Psi''(0, k)}{ik}. \quad (41)$$

Hence, since $U'(0) = 3$,

$$\tau \approx 1 - s + \int_{-\infty}^{\infty} K(x - \xi) s'(\xi) d\xi. \quad (42)$$

We now need to find a solution to the Fourier transform of the Orr-Sommerfeld equation (37) subject to the boundary conditions (38). Then the convolution kernel K and hence the basal shear stress τ will be fully determined. It is not possible to find an exact solution but the largeness of the turbulent Reynolds number Re_T can be exploited to find an approximate analytic expression for $\Psi''(0, k)$. The turbulent Reynolds number can be estimated using (22) to be $\text{Re}_T \approx \frac{3}{f}$; for a typical value of $f \approx 0.005$, we have $\text{Re}_T \approx 600$. The asymptotic solution at large Reynolds number to the Orr-Sommerfeld equation is a well-known problem and the details can be found in Drazin and Reid [7], for example. Thus we do not present the details here; however, an outline of the argument is presented in the appendix for reference. The result can be derived because of the presence of a boundary layer of size $\text{Re}_T^{-1/3}$ just above the sediment layer.

It is ultimately found that

$$\Psi''(0, k) = -\frac{3^{2/3}(ik)^{1/3}\text{Re}_T^{1/3}}{\Gamma(\frac{2}{3})} \quad (43)$$

and so

$$\hat{K}(k) = \frac{3^{2/3} \text{Re}_T^{1/3}}{(ik)^{2/3} \Gamma(\frac{2}{3})} \quad (44)$$

follows from (41). Charru and Hinch [20] and Vincent and Langlois [17] have found a similar relation in their work. To complete the derivation we must find the inverse transform of \hat{K} . Doing so yields

$$K(x) = \begin{cases} \mu x^{-1/3}, & x > 0, \\ 0, & x \leq 0, \end{cases} \quad (45)$$

where

$$\mu = \frac{3^{2/3} \text{Re}_T^{1/3}}{\{\Gamma(\frac{2}{3})\}^2}. \quad (46)$$

For a value of $\text{Re}_T = 600$, and since $\Gamma(\frac{2}{3}) = 1.354$, we find $\mu = 9.57$. Consequently,

$$\tau \approx 1 - s + \mu \int_0^\infty \frac{s'(x - \xi)}{\xi^{1/3}} d\xi. \quad (47)$$

Note that the integral term is proportional to the fractional ($\frac{1}{3}$) derivative of s .

(47) gives the corrected stress under the restrictive assumption that the flow rate, and thus also the eddy viscosity, is constant. The term in s is slightly anomalous, insofar as it suggests that a change in depth only will change the stress, in contradiction to the turbulent friction law (4). To resolve this, suppose that s is constant; we write the stress in (47) in the dimensional form

$$\tau^* = \frac{3\rho_f^* \nu_T^* u_0^*}{h_0^*} \left(1 - \frac{\Delta h}{h_0^*}\right) \approx \frac{3\rho_f^* \nu_T^* u_0^*}{h_0^* + \Delta h}, \quad (48)$$

where $s = \frac{\Delta h}{h_0^*}$; however, since $\nu_T^* \propto h_0^*$, we see that in fact the change in depth in the denominator is compensated by the change to the eddy viscosity. The implication is that the bed perturbation in (47) has zero spatial mean, which is in fact implicit in the solution of the Orr-Sommerfeld equation by use of the Fourier transform.

If we now allow the mean (dimensionless) velocity to vary, then the generalisation of (47) is

$$\tau \approx \bar{u}^2 \left[1 - s + \mu \int_0^\infty \frac{s'(x - \xi)}{\xi^{1/3}} d\xi\right]. \quad (49)$$

4 Linear stability analysis

We now perform a linear stability analysis of the governing equations using the model (47) for the basal shear stress. The governing equations are, from (9) and (28),

$$h = 1 - s; \quad (50)$$

the Exner equation (10),

$$s_t + q_x = 0; \quad (51)$$

the flux, following from (15) with $\varepsilon = 0$ (and omitting the overbar on \bar{u}):

$$hu = 1; \quad (52)$$

the Meyer-Peter and Müller [21] law (11)

$$q = \tau^{3/2}; \quad (53)$$

and the basal shear stress prescription (49),

$$\tau = u^2(1 - s + K * s_x), \quad (54)$$

where $K * s_x$ represents the convolution. The Exner equation can be written as

$$s_t + q'(\tau)\tau_x = 0; \quad (55)$$

after linearising for small bed height s , we therefore find

$$s_t + q'(1)(s_x + K * s_{xx}) = 0. \quad (56)$$

Seeking normal modes of the form $s = s_0 = e^{\sigma t + i k x}$ yields a growth rate given by

$$\text{Re } \sigma = q'(1)k^2 \text{Re } \hat{K}, \quad (57)$$

and using (44) with $q'(1) = \frac{3}{2}$, we find

$$\text{Re } \sigma = \alpha k^{4/3} > 0, \quad (58)$$

where

$$\alpha = \frac{3}{4}c, \quad c = \frac{3^{2/3} \text{Re } T^{1/3}}{\Gamma(\frac{2}{3})}, \quad (59)$$

and the wave speed is

$$-\frac{\text{Im } \sigma}{k} = \frac{3}{2} \left(\frac{\sqrt{3}}{2} c k^{1/3} + 1 \right), \quad (60)$$

implying that the disturbances grow and propagate downstream. Observe that $\text{Re } \sigma \propto k^{4/3}$ so that the growth rate of the disturbances is unbounded for large wavenumbers (or small wavelengths). This problem also occurs in the Kennedy model [14]. The large wavenumber disturbances can be stabilised in this model as described below.

4.1 Stabilisation of large k instabilities

So far, the effect of gravity on the bedload particles has been neglected. Its inclusion leads to a stabilising effect on large wavenumber disturbances as follows.

A particle of diameter D_s^* has a force exerted on it by the flow of approximately $\tau^* D_s^{*2}$ and if the particle is on a (small) slope s_x there is a downstream force due to gravity of approximately $-\Delta\rho^* g^* D_s^{*3} s_x$, where $\Delta\rho^* = \rho_s^* - \rho_f^*$, which must be added to the stress τ^* in order to provide the effective stress τ_e^* on the particle. In dimensionless terms, the consequent effective stress is

$$\tau_e = \tau - \beta s_x, \quad (61)$$

where

$$\beta = \frac{\Delta\rho^* g^* D_s^*}{\rho_f^* f^* u_0^{*2}}. \quad (62)$$

The Exner equation is then

$$\frac{\partial s}{\partial t} + \frac{\partial q(\tau_e)}{\partial x} = 0, \quad (63)$$

and when linearised, equation (56) is modified to

$$s_t + q'(1)(s_x + K * s_{xx} - \beta s_{xx}) = 0. \quad (64)$$

The growth rate thus becomes

$$\text{Re } \sigma = \alpha k^{4/3} - \frac{3}{2}\beta k^2. \quad (65)$$

Thus the effect of gravity is to stabilise the short wavelength disturbances, but the large wavelength disturbances are preserved. The maximum growth rate occurs when

$$k = k_{\max} = \left(\frac{4\alpha}{9\beta}\right)^{3/2}, \quad (66)$$

and from (59), we have $c \approx 12.96$ when $\text{Re}_T = 600$, and thus $\alpha \approx 9.72$. Using typical values for air flow over sand of $\frac{\Delta\rho^*}{\rho_f^*} = 2.17 \times 10^3$, $g^* = 9.8 \text{ m s}^{-2}$, $D_s^* = 10^{-4} \text{ m}$, $f^* = 0.005$ and $u_0^* = 10 \text{ m s}^{-1}$, we find $\beta \approx 4.3$, and thus $k_{\max} \approx 1.04$.¹ In dimensional terms the fastest growing wavelength is

$$\lambda^* = \frac{2\pi h_0^*}{k_{\max}}, \quad (67)$$

which is approximately 3.6 km if we take $h_0^* = 600 \text{ m}$. Generally, the predicted wavelength is about six times the flow depth.

5 Separation

The evolution equation for dunes is given by the Exner equation

$$s_t + q_x = 0, \quad (68)$$

where $q = q(\tau_e)$, and the effective shear stress is given by

$$\tau_e = \tau - \beta s_x, \quad \tau = \frac{1}{(1-s)^2}(1-s + K * s_x). \quad (69)$$

Although the computation of the shear stress is based on a linearisation of the flow equations, the evolution equation for s provides a fully nonlinear model for s . Fowler [10], [9] developed a mildly nonlinear evolution equation from (68) by linearising it as

$$\frac{\partial s}{\partial t} + q'(1) \frac{\partial \tau_e}{\partial x} = 0, \quad (70)$$

and writing the effective shear stress as

$$\tau_e \approx 1 + s + s^2 + K * s_x - \beta s_x. \quad (71)$$

¹Note that $\frac{1}{\beta}$ is the Shields stress, which must be greater than approximately 0.05 for sediment transport to occur, i. e., $\beta \lesssim 20$.

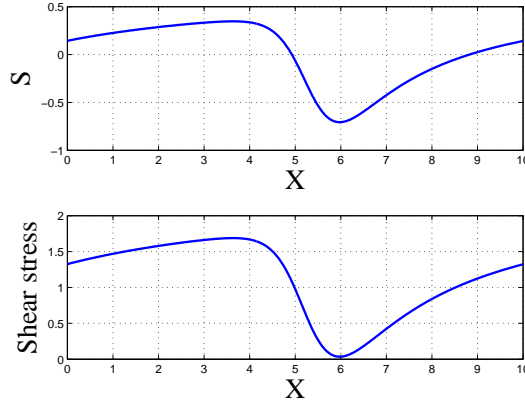


Figure 2: Solution of (72) at large times. A single wave occupies the whole computation domain.

With a suitable change of variable together with a mild rescaling, we can derive the evolution equation in the form

$$\frac{\partial s}{\partial \tau} + \frac{\partial}{\partial \xi} \left[\frac{1}{2} s^2 + \int_0^\infty \frac{1}{\eta^{1/3}} \frac{\partial s(\xi - \eta)}{\partial \xi} d\eta - \frac{\partial s}{\partial \xi} \right] = 0. \quad (72)$$

Solutions of (72) have the following behaviour, when solved numerically with periodic boundary conditions. An initially almost flat state grows into a series of waves, whose wavelength coarsens until eventually a single wave occupies the domain. The wave has a steep lee side, much like a dune, although there is no separation in the model. To understand this behaviour, we note that for large wavelengths, the model (72) approaches Burgers' equation, with a small diffusivity. Thus the solution evolves to a series of shocks, and the coarsening is a consequence of the larger shock catching and engulfing the smaller shocks. The integral term also becomes small in this limit, and its primary purpose appears to be to generate the instability of the uniform state.

Since both the diffusive and the integral term become small at large time, it might be expected that (71) would provide a good approximation to (69). Further thought suggests that this may not in fact be the case. The solution in figure 2 has large amplitude and slope, suggesting that in reality, separation will occur when the shear stress reaches zero, and a slip face will occur if the slope reaches that corresponding to the angle of repose $\phi \approx 34^\circ$, i. e., $-s_x > S_c = \tan \phi \approx 0.67$. Figure 3 shows a numerical solution of the full model (68) with (69), starting from the nearly flat state. As the waves grow, the slopes increase, and also the minimum shear stress decreases, until at some point separation occurs because τ reaches zero.

5.1 A model for separation

As discussed in the introduction, once separation occurs, the computation of the shear stress must be rethought, and this applies both to the Benjamin model as adopted here, and the Jackson-Hunt model used by Kroy *et al.* [16]. In the present paper, we do not address this issue, but assume that τ is still given by (69), even when separation occurs. We do, however, address the issue of how to compute the solution when separation occurs.

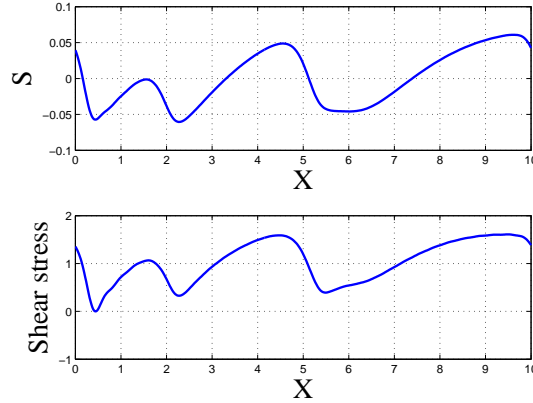


Figure 3: Solution of (68) using (69), together with $q(\tau) = \tau^{3/2}$, at the point where the shear stress first reaches zero.

One way to do this is to realise that the Exner equation becomes redundant when τ reaches zero, and this can be used to effect a solution, by retaining the Exner equation, but defining the function q to be such that τ remains at zero. If, first, we suppose $\beta = 0$, then we define q as the graph

$$\begin{aligned} q &= q_0(\tau), & \tau > 0, \\ q &> 0, & \tau = 0. \end{aligned} \quad (73)$$

The solution of this automatically caters for separation.

When attempting to solve the Exner equation numerically, it is expeditious to approximate (73). For example, if $q_0 = \tau^{3/2}$, then we might choose

$$q = [\tau]_+^{3/2} + \frac{\delta_1}{\tau + \delta_2}, \quad (74)$$

where δ_1 and δ_2 are suitably small positive constants. If β is non-zero, then we need to allow it to be variable in such a way that $\beta \rightarrow 0$ as $\tau \rightarrow 0$. This can be achieved by allowing

$$\beta = \beta_0 [1 - \exp(-\Lambda_1 \tau)], \quad (75)$$

where Λ_1 is large.

Numerically, (75) is inadvisable, since the spectral method that we use will allow transients in which τ and thus $\beta < 0$; this can be avoided by the alternative choice

$$\beta = \beta_0 [1 + \tanh \Lambda_1 (\tau - \delta_3)], \quad (76)$$

and we use this in the computations shown in figures 4, 5 and 6. Figure 4 shows the steady state solution at large time. The apparent Gibbs oscillations are then removed by taking a moving average over an interval $\Delta = 16\delta x$ where $\delta x = 0.0196$ is the computational grid spacing. Thus $\Delta \approx 0.314$. The smoothed solution is shown in figure 5. A solution at early time ($t = 0.025$) is also shown, see figure 6.

Finally we observe that also we should enable infinite q if $-s_x$ reaches S_c , in order that slopes do not exceed the angle of repose. In practice we found, however, that the maximum slope never approaches the angle of repose, so no modification needed to be included for this.

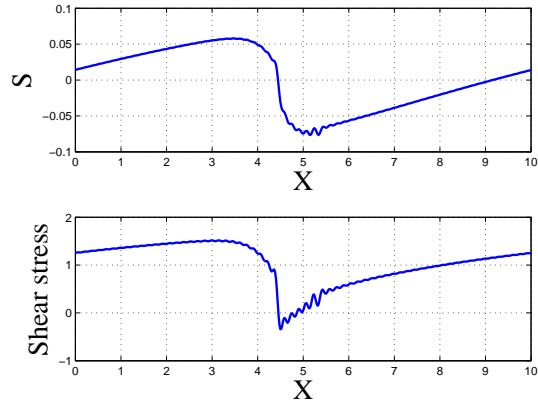


Figure 4: Solution of (68) using (74), with values $\delta_1 = 0.25$, $\delta_2 = 0.25$, $\delta_3 = 0.5$, and also (76), with $\Lambda_1 = 5$. The sand surface in the separation bubble is taken to consist of a slip face from the crest of the dune, together with a horizontal surface up to the point of flow reattachment. The solution can be smoothed by taking a moving average, see figure 5

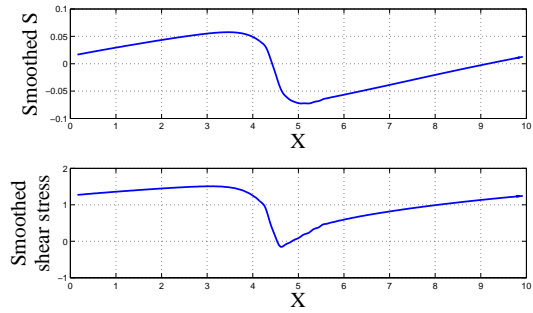


Figure 5: The solution shown in 4 after a moving average has been taken. The interval over which the average is taken is $\Delta = 16\delta x$, where $\delta x = 0.0196$ is the grid spacing.

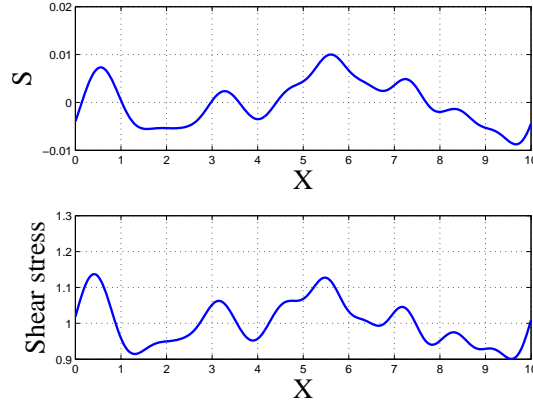


Figure 6: Solution of (68) using (74), with values $\delta_1 = 0.25$, $\delta_2 = 0.25$, $\delta_3 = 0.5$, and also (76), with $\Lambda_1 = 5$ shown for early time, $t = 0.025$. The initial condition is a randomly perturbed bed.

6 Conclusions

We have provided a derivation of the Exner-Benjamin model of dune formation, in which it is assumed that the air or water flow is described by a constant eddy viscosity. If the model is solved in a mildly nonlinear formulation, coarsening occurs, but in practice separation will occur before this. We have shown how the model, using the same formula for the derived shear stress, can be extended computationally to allow for the effects of separation. However, we also point out that a second modification of the theory is necessary, and this is that the expression for the shear stress itself must take account of the flow separation. No theory of dune formation has as yet addressed this issue, and we reserve its resolution to a future paper.

Model computations using the present approach show that a separation bubble inevitably occurs, and that the resulting dunes obtain a finite elevation, and propagate forwards at a finite rate. As is the case for the model without separation, coarsening occurs, and the initial dunes coalesce, so that eventually a single dune fills the domain, as shown in figure 4. For the computation shown in figure 4, the elevation is 34.8 m and the dune speed is 11.95 m a^{-1} , assuming the aeolian parameter values used earlier.

Acknowledgements

This publication is based on work supported by Award No. KUK-C1-013-04, made by King Abdullah University of Science and Technology (KAUST). A. C. F. acknowledges the support of the Mathematics Applications Consortium for Science and Industry (www.macsi.ul.ie) funded by the Science Foundation Ireland mathematics initiative grant 06/MI/005. A. S. E. thanks Andreas Baas, Giles Wiggs, John Hinch, John Ockendon, Ian Hewitt and Chris Cawthorn for many useful conversations.

Appendix. Asymptotics of Orr-Sommerfeld equation

In this appendix we present some of the details of the asymptotic solution of the Orr-Sommerfeld equation, which provides us with an approximate expression for the term $\Psi''(0, k)$ that is required in order to fully derive the formula for the basal shear stress. This analysis is well known (see Drazin and Reid [7]) but is included here for completeness.

We consider equation (37) subject to (38) in the limit $\text{Re}_T \rightarrow \infty$. The outer solution is expanded in powers of Re_T^{-1} :

$$\Psi \sim \text{Re}_T^{-m} (\Psi_0 + \text{Re}_T^{-1} \Psi_1 + O(\text{Re}_T^{-2})), \quad (77)$$

where m is determined below. The equation for Ψ_0 is the Rayleigh equation,

$$U(\Psi_0'' - k^2 \Psi_0) - U'' \Psi_0 = 0. \quad (78)$$

Clearly, this is a singular perturbation problem: the no slip condition at $z = 0$ cannot be satisfied and a boundary layer is introduced below. The Rayleigh equation is solved by Frobenius's method; linearly independent solutions of the form

$$\psi_1(z) = \sum_{n=0}^{\infty} a_n z^n \quad (79)$$

and

$$\psi_2(z) = \sum_{n=0}^{\infty} b_n z^n - \psi_1 \log(z) \quad (80)$$

are sought. The coefficients a_n and b_n are found to satisfy the recurrence relations

$$a_n = \frac{1}{n(n-1)} \left(\frac{1}{2} n(n-3) a_{n-1} + k^2 a_{n-2} - \frac{1}{2} k^2 a_{n-3} \right) \quad (81)$$

and

$$b_n = \frac{1}{n(n-1)} \left(\frac{1}{2} n(n-3) b_{n-1} + k^2 b_{n-2} - \frac{1}{2} k^2 b_{n-3} + \frac{1}{2} (2n-3) a_{n-1} - (2n-1) a_n \right), \quad (82)$$

and $a_0 = 0$, $a_1 = 1$, $a_2 = -\frac{1}{2}$; $b_0 = 1$, $b_1 = 0$ and $b_2 = \frac{1}{2} k^2 - 1$. In order to satisfy the boundary condition $\Psi_0(1) = 0$ we suppose that $\Psi_0(z)$ is a linear combination of the two series, i.e.

$$\Psi_0(z) = \beta \left(\psi_2(z) - \frac{\psi_2(1)}{\psi_1(1)} \psi_1(z) \right). \quad (83)$$

As $z \rightarrow 0$, $\Psi \rightarrow \beta \text{Re}_T^{-m}$; the boundary condition at $z = 0$ is not satisfied and we need to introduce a boundary layer, as stated above. The z co-ordinate is rescaled by writing $z = \varepsilon Z$. Then $U(\varepsilon Z) = U(0) + \varepsilon Z U'(0) + O(\varepsilon^2)$ and $U''(\varepsilon Z) = U''(0) + \varepsilon Z U'''(0) + O(\varepsilon^2)$. If we balance the leading order terms after substitution into equation (37) we discover that

$$\varepsilon = [(ik)U'(0)\text{Re}_T]^{-1/3}, \quad (84)$$

and the inner equation is

$$\Psi^{(4)} - Z\Psi'' + \frac{\varepsilon}{2} \left(\frac{Z^2}{2}\Psi'' - \Psi \right) = O(\varepsilon^2). \quad (85)$$

We then write an inner expansion as

$$\Psi = \text{Re}_T^{-m} (\Phi_0 + \varepsilon\Phi_1 + O(\varepsilon^2)) \quad (86)$$

which produces

$$\Phi_0^{(4)} - Z\Phi_0'' = 0 \quad (87)$$

and

$$\Phi_1^{(4)} - Z\Phi_1'' = \Phi_0 - \frac{Z^2}{2}\Phi_0''. \quad (88)$$

Equation (87) is Airy's equation for Φ_0'' . From Drazin and Reid [7], Φ_0 is given by

$$\Phi_0 = \alpha_0 + \alpha_1 Z + \alpha_2 A_2^{(1)}(Z) + \alpha_3 A_2^{(3)}(Z) \quad (89)$$

where α_i are constants and $A_p^{(k)}(Z)$ are the generalised Airy functions given by

$$A_p^{(k)}(Z) = \frac{1}{2\pi i} \int_{L_k} t^{-p} e^{ZT - \frac{1}{3}t^3} dt, \quad (90)$$

with L_k being various contours in the complex plane. Matching the solution for Ψ_0 as $z \rightarrow 0$ with the solution for Φ_0 as $\varepsilon Z \rightarrow \infty$ yields $\beta = \alpha_0$, $\alpha_1 = 0$ and $\alpha_3 = 0$. The remaining constants are determined by the boundary conditions $\Psi(0) = 0$ and $\varepsilon^{-1}\Psi_Z(Z=0) = 1$ yielding

$$\alpha_2 = -\frac{\beta}{A_2^{(1)}(0)}, \quad \beta = -\frac{\varepsilon \text{Re}_T^m A_2^{(1)}(0)}{A_1^{(1)}(0)}. \quad (91)$$

Therefore the inner solution is

$$\Psi \sim \frac{\varepsilon}{A_1^{(1)}(0)} \left[A_2^{(1)}(Z) - A_2^{(1)}(0) \right] + O(\varepsilon^2) \quad (92)$$

and the outer solution is

$$\Psi \sim -\frac{\varepsilon A_2^{(1)}(0)}{A_1^{(1)}(0)} \left[\psi_2(z) - \frac{\psi_2(1)}{\psi_1(1)} \psi_1(z) \right] + O(\varepsilon^2). \quad (93)$$

It is now possible to determine the exponent m . Implicitly, β is assumed to be order one. Recalling (84) which states $\text{Re}_T \propto \varepsilon^{-3}$ we see that $m = 1/3$ in order for the above expression to be order unity. To finally determine $\Psi_{zz}(z=0)$ we must find the second derivative of the inner solution. This turns out to be

$$\Psi_{zz}|_{z=0} = -\frac{3^{2/3}(ik)^{1/3} \text{Re}_T^{1/3}}{\Gamma(\frac{2}{3})} \quad (94)$$

where we have used the fact that $A_1^{(1)}(0) = -\frac{1}{3}$ and the fact that $A_0^{(1)}(0) = \frac{1}{3^{2/3}\Gamma(\frac{2}{3})}$.

References

- [1] Andreotti, B., Claudin, P., and Douady, S. Selection of dune shapes and velocities. part 2: a two-dimensional modelling. *Eur. Phys. J. B*, 28:341–352, 2002.
- [2] Bagnold, R. A. *The Physics of Blown Sand and Desert Dunes*. Chapman and Hal, 1971.
- [3] Benjamin, T. B. Shearing flow over a wavy boundary. *J. Fluid Mech.*, 6:161–205, 1959.
- [4] Charru, F. and Hinch, E. J. Ripple formation on a particle bed sheared by a viscous liquid. Part 1. Steady flow. *J. Fluid Mech.*, 550:111–121, 2006.
- [5] Colombini, M. Revisiting the linear theory of sand dune formation. *J. Fluid Mech.*, 502:1–16, 2004.
- [6] Dong, Z., Liu, X., Wang H., and Wang X. Aeolian sand transport: a wind tunnel model. *Sedimentary Geology*, 161(1-2):71–83, 2003.
- [7] Drazin, P. G., and Reid W. H. *Hydrodynamic stability*. Cambridge University Press, 1981.
- [8] Englund, F. Instability of erodible beds. *J. Fluid Mech.*, 42(2):225–244, 1970.
- [9] Fowler, A. C. Evolution equations for dunes and drumlins. *Revista de la Real Academia Ciencias Exactas, Fisicas y Naturales, Serie A. Mat*, 96(3):377–387, 2002.
- [10] Fowler, A.C. Dunes and drumlins. In Provenzale, A. and Balmforth, N., editors, *Geomorphological fluid dynamics*, pages 430–454. Springer-Verlag, Berlin, 2001.
- [11] Fredsøe, J. On the development of dunes in erodible channels. *J Fluid Mech.*, 64:1–16, 1974.
- [12] Hunt, J. C. R., Leibovich, S., and Richards, K. J. Turbulent shear flows over low hills. *Quart. J. Roy. Met. Soc.*, 114:1435–1470, 1988.
- [13] Jackson, P. S. and Hunt, J. C. R. Turbulent wind flow over a low hill. *Q. J. R. Meterol. Soc.*, 101:929–955, 1975.
- [14] Kennedy, J. F. The mechanics of dunes and anti-dunes in erodible bed channels. *J. Fluid Mech.*, 16:521–544, 1963.
- [15] Kouakou, K. K. J. and Lagrée, P-Y. Evolution of a model dune in a shear flow. *Eur. J. Mech. B*, 25:348–359, 2006.
- [16] Kroy, K., Sauermann, G., and Hermann, H. J. Minimal model for sand dunes. *Phys. Rev. Letts.*, 88(5):1–4, 2002.
- [17] Langlois, V. and Valance, A. Formation of two-dimensional sand ripples under laminar shear flow. *Phys. Rev. Letts.*, 94:248001, 2005.
- [18] Langlois, V. and Valance, A. Three-dimensionality of sand ripples under steady laminar shear flow. *J. Geophys. Res.*, 110, 2005.
- [19] Langlois, V. and Valance, A. Initiation and evolution of current ripples on a flat sand bed under turbulent water flow. *European Physical Journal E*, 22:201–208, 2007.
- [20] Larrieu, E., Hinch, E. J., and Charru, F. Lagrangian drift near a wavy boundary in a viscous oscillating flow. *Under consideration for publication in J. Fluid Mech.*, 2009.

- [21] Meyer-Peter, E. and Muller, R. Formulas for bed-load transport. *Proc. Int. Assoc. Hydraul. Res., 3rd annual conference, Stockholm*, pages 39–64, 1948.
- [22] Ouriemi, M., Aussillous, P., and Guazelli, E. Sediment dynamics. part2. dune formation in pipe flow. *Under consideration for publication in J. Fluid Mech.*, 2009.
- [23] Parsons, D. R., Walker, I. J., and Wiggs, G. F. S. Numerical modelling of flow structures over idealized transverse aeolian dunes of varying geometry. *Geomorphology*, 59:149–164, 2004.
- [24] Parsons, D. R., Wiggs, G. F. S., Walker, I.J., Ferguson, R. I., and Garvey, B. G. Numerical modelling of airflow over an idealised transverse dune. *Environmental Modelling and Software*, 19:153–162, 2004.
- [25] Parteli, E. J. R., Dúran, O., and Herrmann, H. J. Minimal size of a barchan dune. *Phys. Rev. E*, 75(1):011301, 2007.
- [26] Parteli, E.J.R., Durán, O., Tsoar, H., Schwämmle, V. and Herrmann, H. J. Dune formation under bimodal winds. *Proc. Nat. Acad. Sci.*, 106:22085 – 22089, 2009.
- [27] Richards, K. J. The formation of ripples and dunes on an erodible bed. *J. Fluid Mech.*, 99:597 – 618, 1980.
- [28] Sauermann, G., Kroy, K., and Herrmann, H. J. Continuum saltation model for sand dunes. *Phys. Rev. E*, 64, 2001.
- [29] Schämmle, V. and Herrmann, H. J. Modelling transverse dunes. <http://www.citebase.org/abstract?id=oai:arXiv.org:cond-mat/0301589>, 2003.
- [30] Smith, F. T. Laminar flow over a small hump on a flat plate. *J. Fluid Mech.*, 57:803–824, 1973.
- [31] Smith, J. D. Stability of a sand bed subjected to a shear flow of low froude number. *J. Geophys. Res*, 75(30):5928–5940, 1970.
- [32] Sumer, B. M. and Bakioglu, M. On the formation of ripples on an erodible bed. *J. Fluid Mech.*, 144:177–190, 1984.
- [33] Valance, A. and Langlois, V. Ripple formation over a sand bed submitted to a laminar shear flow. *European Physical Journal B.*, 43:283–294, 2005.

RECENT REPORTS

02/10	Determining the equation of state of highly plasticised metals from boundary velocimetry	Hinch
03/10	Stability of bumps in piecewise smooth neural elds with nonlinear adaptation	Kilpatrick Bressloff
04/10	Random intermittent search and the tug-of-war model of motor-driven transport	Newby Bressloff
05/10	Ergodic directional switching in mobile insect groups	Escudero <i>et al.</i>
06/10	Derivation of a dual porosity model for the uptake of nutrients by root hairs	Zygalakis Roose
07/10	Frost heave in compressible soils	Majumdar Peppin Style Sander
08/10	A volume-preserving sharpening approach for the propagation of sharp phase boundaries in multiphase lattice Boltzmann simulations	Reis Dellar
09/10	Anticavitation and differential growth in elastic shells	Moulton Goriely
10/10	On the mechanical stability of growing arteries	Goriely Vandiver
11/10	Nonlinear Correction to the Euler Buckling Formula for Compressible Cylinders	De Pascalis Destrade Goriely
12/10	Nonlinear Morphoelastic Plates I: Genesis of Residual Stress	McMahon Goriely Tabor
13/10	Nonlinear Morphoelastic Plates II: Exodus to Buckled States	McMahon Goriely Tabor
14/10	Analysis of Brownian dynamics simulations of reversible biomolecular reactions	Lipkova Zygalakis Chapman Erban
15/10	Travelling waves in hyperbolic chemotaxis equations	Xue Hwang Painter Erban
16/10	The Physics and Mechanics of Biological Systems	Goriely Moulton
17/10	Crust formation in drying colloidal suspensions	Style Peppin

18/10	A Mathematical Model of Tumor-Immune Interactions	Robertson-Tessi El-Kareh Goriely
19/10	Elastic cavitation, tube hollowing, and differential growth in plants and biological tissues	Goriely Moulton Vandiver
20/10	Asymptotic expressions for the nearest and furthest dislocations in a pile-up against a grain boundary	Hall
21/10	Cardiac electromechanics: the effect of contraction model on the mathematical problem and accuracy of the numerical scheme	Pathmanathan Chapman Gavaghan Whiteley
22/10	Fat vs. thin threading approach on GPUs: application to stochastic simulation of chemical reactions	Klingbeil Erban Giles Maini
23/10	Asymptotic analysis of a system of algebraic equations arising in dislocation theory	Hall Chapman Ockendon
25/10	Preconditioning for Allen-Cahn Variational Inequalities with Non-Local Constraints	Blank Sarbu Stoll

Copies of these, and any other OCCAM reports can be obtained from:

**Oxford Centre for Collaborative Applied Mathematics
Mathematical Institute
24 - 29 St Giles'
Oxford
OX1 3LB
England**

www.maths.ox.ac.uk/occam